Opto-Electronic Discovery

Review

2026, Vol. , No.

Open Access

Optical sensing-based cytological image analysis enhanced with artificial intelligence: a review

Jiuchuan Guo[1], Ziyan Yin[1], Lanqing Zeng[1], Hongyu Li[1], Yusheng Fu[1], Renting Liu[1] and Jinhong Guo[2]*

Abstract: Optical sensing technology is essential in cytological image analysis, particularly for cell morphology studies. Advancements in optical microscopy, such as bright-field, fluorescence, and confocal microscopy, have improved image resolution and acquisition speed, aiding early disease diagnosis. However, as sample volume and data complexity grow, traditional manual analysis struggles with efficiency and accuracy. Artificial intelligence (AI) is rapidly becoming a main method for automatic medical image analysis due to its powerful learning ability and pattern processing capability. Since cytology contributes greatly to early disease diagnosis and pathological assessment, recent research has focused on training AI for better utilization in intelligent cytological image analysis and received remarkable success. To provide a systematic and comprehensive understanding of the latest research progress, this paper reviews and summarizes AI methods applied in this field, including a detailed discussion on feature extraction methods (e.g., extraction of morphological features and color features of cells), segmentation methods (e.g., nucleus and parasite segmentation), detection methods (e.g., blood cell detection), classification methods (e.g., benign vs. malignant cell classification) and future challenge. This is followed by an overview of the application and development of artificial intelligence in detecting specific diseases, using research samples as a guide. Finally, the various challenges facing the field of intelligent analysis of cytological images, including problems from the lack of data sets, method selection, and clinical applications, are discussed in detail, and solutions that have proven to be informative and more promising are provided. By summarizing the latest solutions, this paper hopes to provide new ideas to address the imbalances in the development of cytological AI and the effective development of new methods in similar fields.

Keywords: digital pathology; cytopathology; blood; artificial intelligence; deep learning; computer-aided detection

DOI: 10.67704/oed.2026.250001

Citation: Guo JC, Yin ZY, Zeng LQ et al. Optical sensing-based cytological image analysis enhanced with artificial intelligence: a review. *Opto-Electron Discov*, 250001 (2026).

Introduction

Cytology is a discipline that involves the identification and morphological analysis of cells using light microscopy to aid pathological diagnosis[1]. It is widely used in the examination of common and fatal cancers in the human body, including lung, pancreatic, breast, and thyroid cancers, and other viral diseases and inflammatory[2]. Samples for cytology analysis can be obtained in a variety of ways, including fine-needle aspiration (FNA), body fluids, and naturally shed cells[3]. Compared with histology which requires anesthesia and biopsy[4], cytology proves to be cost-effective and non-invasive.

With the rapid advancement of biomedical imaging, especially in optical sensing technologies, cytological imaging has entered the era of high-resolution, high-throughput data acquisition. Techniques such as bright-field microscopy, fluorescence microscopy, and whole slide imaging (WSI) have significantly improved the quality and depth of cellular visualization. However, the increasing volume and complexity of image data have also introduced new challenges, including diagnostic subjectivity, time-consuming manual review, and higher misdiagnosis risks.

To address these issues, artificial intelligence (AI) has

Received: 10 September 2025

Accepted: 17 November 2025

Published online: 29 January 2026

[1]University of Electronic Science and Technology of China, Chengdu 611731, China; [2]School of Automation and Intelligent Sensing, Shanghai Jiaotong University, Shanghai 200240, China.
*Correspondence: JH Guo, E-mail: guojinhong@sjtu.edu.cn

emerged as a powerful tool to enhance cytological image analysis. By integrating optical sensing with AI-driven approaches such as computer-aided detection (CAD), deep learning-based classification, and automated specimen recognition, researchers aim to improve diagnostic efficiency, reproducibility, and accuracy.

This review focuses on the synergistic application of optical sensing and AI technologies in cytological image analysis. Beginning with a discussion of key optical modalities, we summarize recent progress in AI-enhanced image interpretation across twelve representative cytological sample types. We further analyze the current limitations, technical bottlenecks, and emerging solutions within this interdisciplinary field. By providing a structured and up-to-date overview, this review seeks to inform and inspire researchers, ultimately accelerating the digital and intelligent transformation of cytological diagnostics. The structure of this article is illustrated in Fig. 1.

Optical sensing technique

Conventional microscopy

Optical sensing plays a fundamental role in cytological image analysis by enabling the acquisition of high-resolution, real-time, and non-invasive cellular images. Since cytology centers on the observation and interpretation of cellular morphology, structure, and behavior, the quality of image data is crucial for accurate analysis and diagnosis. Optical imaging modalities, such as bright-field, fluorescence, and confocal microscopy, provide the necessary spatial and temporal resolution to capture detailed cellular features, including nucleus size, cytoplasmic texture, and subcellular structures.

Bright-field microscopy is the most widely used imaging technique, relying on transmitted light to visualize stained cellular samples. Ma et al[5]. proposed a spatially-incoherent annular illumination microscopy (SAIM) method by modifying bright-field microscopes with an annular LED array, achieving real-time, non-fluorescent optical sectioning with 150 nm lateral and 600 nm axial resolution. Gutiérrez-Medina et al[6]. developed an optical sectioning in bright-field microscopy (OSBM) method using coherent Köhler illumination and a digital filtering pipeline, enabling 3D reconstruction of unlabeled samples without additional hardware or modeling.

Fluorescence microscopy enables selective imaging of specific cellular structures or biomolecules through the excitation of fluorescent dyes. Chen et al[7]. proposed a high-speed large-field multifocal illumination (LMI) fluorescence microscopy technique by combining a beam-splitting grating and an acousto-optic deflector, enabling real-time, centimeter-scale imaging with improved resolution and depth of focus for in vivo vascular dynamics. Zhang et al[8]. proposed an LED-based multicolor extended resolution transmission fluorescence microscopy system utilizing a programmable LED array and a simple diffraction grating unit, which solved the problems of high cost and complexity in traditional multicolor structured illumination microscopy (SIM) and enabled compact, cost-effective multicolor extended resolution imaging of biological tissues such as mouse kidney sections.

Super-resolution techniques such as stimulated emission depletion(STED), photoactivation localization microscopy

Fig. 1 | Overview of AI-based automated cytological image analysis.

(PALM), and stochastic optical reconstruction microscopy (STORM) overcome the diffraction limit to achieve nanometer-scale resolution. Kim et al[9]. developed a grating-based spectrally resolved STORM (SR-STORM) system combined with the solvatochromic dye Nile red, which solved the limitations of complex optics and low spectral resolution in prism-based SR-STORM and enabled nanoscale polarity sensing of functional groups within surfactant molecules at the single-molecule level.

Overall, different optical imaging modalities offer complementary strengths in cytological imaging. Bright-field microscopy remains the most cost-effective and widely used technique for routine cell observation but requires staining and provides limited contrast for transparent samples. Fluorescence microscopy enables highly specific molecular visualization at the expense of complex labeling and higher instrumentation cost. Super-resolution techniques, such as STED, PALM, and STORM, achieve nanometer-scale resolution but are limited by slow acquisition speed, photobleaching, and system complexity. In comparison, emerging label-free methods, including QPI, HSI, and Raman imaging discussed in subsequent sections, provide quantitative, non-destructive, and high-content imaging capabilities that further expand the analytical potential of cytological diagnostics.

Quantitative phase imaging

Quantitative Phase Imaging (QPI) is a label-free optical technique that measures the optical path difference caused by variations in the refractive index of transparent biological samples[10]. Unlike conventional microscopy that relies on staining, QPI enables precise quantification of cellular morphology and dynamics in a non-destructive manner. It has been widely applied in cytology for detecting and classifying morphological differences between normal and abnormal cells, facilitating early disease diagnosis.

In the context of endoscopic miniaturization, Sun et al[11]. recently demonstrated a deep learning–based approach for real-time, calibration-free QPI through a multi-core fiber. Their method uses a trained neural network to directly reconstruct phase images from far-field speckles, achieving high-fidelity phase retrieval at 181 frames per second. This overcomes the computational bottleneck of traditional iterative algorithms and eliminates the need for system calibration, paving the way for real-time in vivo phase-contrast endoscopy.

Generative AI, such as generative adversarial networks (GANs), has also been applied to accelerate and enhance QPI reconstruction. For example, Li et al[12]. used a GAN to reconstruct high-fidelity 3D refractive index tomograms in epi-mode qOBM. Their model, requiring only three input planes, achieved a ~9-fold speed increase over traditional methods, showcasing the potential of generative models for real-time, computationally efficient QPI and virtual staining applications.

In addition to software-based deep learning reconstruction, recent studies have explored the integration of AI directly into optical hardware. For instance, Shen et al[13]. developed a multispectral QPI system using a diffractive optical network (DON), which performs all-optical spectral reconstruction by embedding neural computation into diffractive layers. This approach enables label-free, high-throughput phase imaging across multiple wavelengths, representing a promising direction for AI–optics co-design in cytological imaging.

Hyperspectral imaging

Hyperspectral imaging (HSI) is an advanced optical sensing technique that captures both spatial and spectral information simultaneously, generating a three-dimensional data cube in which each pixel contains a full spectral signature[14]. This allows for the characterization of biochemical composition and molecular variations in cells that are invisible to conventional microscopy. Jiao et al[15]. developed a hyperspectral laparoscope combined with an improved U-Net incorporating convolutional down-sampling and attention modules, achieving 97.68% accuracy in identifying metastatic lymph nodes. This demonstrates the strong potential of AI-enhanced HSI systems for label-free intraoperative diagnosis. Yang et al[16]. proposed a dual-branch mapping GAN with transformer (DMTF-GAN) for few-shot hyperspectral image classification, which integrates generative modeling and attention-based spectral learning. The model improves feature representation and classification accuracy under limited data, demonstrating the potential of generative AI in HSI-based cytological analysis.

Furthermore, Zhao et al[17]. provided a comprehensive overview of on-chip AI-powered hyperspectral imaging systems, emphasizing hardware–software co-design strategies for real-time and energy-efficient spectral processing. Their work highlights the use of optical neural networks (ONN) and spiking neural networks (SNN) for intelligent HSI computation, which enable high-throughput, low-power spectral analysis directly at the hardware level. This direction represents the emerging convergence of AI algorithms and optical sensing hardware, paving the way for next-generation intelligent HSI platforms in cytological analysis.

Raman spectroscopic imaging

Raman spectroscopic imaging is a label-free optical technique based on inelastic light scattering, which provides molecular-level information about the biochemical composition of cells and tissues[18]. Each molecule exhibits a unique Raman spectral fingerprint, allowing for the identification of cellular components such as nucleic acids, lipids, and proteins. This technique has been widely applied in cytology

for the detection and classification of normal and abnormal cells, offering a powerful approach for molecular-level diagnosis without staining.

To further improve efficiency, Huang et al[19]. proposed a low-rank constraint–based method to enhance the signal-to-noise ratio and enable rapid discrimination between normal and cancerous tissues. This approach achieved accurate tissue classification while reducing acquisition time by over two orders of magnitude, demonstrating the potential of integrating optimization algorithms with Raman spectroscopy for high-throughput cytological imaging.

Moreover, Horgan et al[20]. developed an image-guided Raman probe-tracking system. This system utilizes a camera and computer vision algorithms to track the position and orientation of a handheld Raman probe in real-time. By spatially co-registering each Raman spectrum with its precise location on the wide-field image, the system can generate an augmented reality map of tissue pathology. This approach effectively transforms pointwise spectroscopic data into a diagnostic image, thereby enabling the detection and delineation of tumor margins on both ex vivo human biopsy samples and in vivo mouse models.

Application of artificial intelligence in cytological image analysis

This section provides a systematic overview of the latest advances in the application of artificial intelligence in cytological image analysis. Cytological image analysis is a methodology that utilizes image processing, computer vision techniques, and artificial intelligence to automatically extract, quantify, and interpret cellular-related information from biological microscopic images. It is primarily used to study the dynamic changes in cell morphology, structure, quantity, and function, as well as their correlation with diseases. As illustrated in Fig. 2, common cytological image analysis methods can be primarily classified into two categories: one based on traditional machine learning, and the other relying on deep learning.

Based on the sources of sample acquisition, we divided cytological samples into four categories: natural shed, body cavity fluid, fine needle aspiration, and others. We selected 12 representative sample types for detailed analysis and visually presented the advanced research in the field of artificial intelligence methods in these areas over the past five years. As different cytological images have both similarities and unique characteristics, we hope to provide readers with a more complete understanding of the research status of intelligent analysis of cytological images through this systematic review. In Table 1, We have provided a detailed description and comparison of existing AI-based image analysis technologies, enabling subsequent researchers to select the most appropriate methods for their research objectives based on the specific characteristics of cytological images.

Natural shed cytology

Naturally eliminated material from the human body is widely used in medical clinical testing. It is an important source of samples for cytological testing because it is easy to collect without the need for additional equipment or surgery, and it reflects the physiological condition of the patient. There is a wide range of such samples, including urine, stool, sputum, semen, etc., whose contents need to be examined to identify the number and morphology of the target cells (such as white blood cells, parasite eggs, tubercu-

Fig. 2 | Artificial intelligence methods for achieving positive performance in cytological image analysis, and a comparison of their pros and cons.

Table 1 | Cytology image information processing method based on artificial intelligence.

Methods	Machine learning-based		Deep learning-based	
Segmentation	Thresholding, morphological operation, watersheds, etc.	**Pros:** simple implementation; small computational effort.	FCN, etc.	**Pros:** enables pixel-level segmentation of images.
		Cons: inability to segment overlapping cells.		**Cons:** insensitive to detail; not enough refinement of segmentation results.
	Active contour models, etc.	**Pros:** good adaptability to complex shapes.	U-Net, etc.	**Pros:** better contextual information dissemination; good performance on small data sets.
		Cons: higher complexity.		**Cons:** duplicate operations exist.
Feature extraction	Color features, shape features, texture features, other features	**Pros:** intuitive; can be optimized based on domain knowledge.	CNN	**Pros:** self-learning; adaptable; more abstract and higher level features.
		Cons: less efficient; important features may be overlooked.		**Cons:** not easily interpretable; computationally demanding.
Classification	KNN, logistic regression, naïve bayes, decision tree, random forest, etc.	**Pros:** fast calculations; easy to interpret and understand.	VGGNet, ResNet, etc.	**Depth:** more abstract features
			Inception, etc.	**Width:** better generalization ability
		Cons: requires manual feature design, difficult to handle complex or unbalanced data.	DenseNet, etc.	**Multipath:** higher robustness
			SqueezeNet, etc.	**Lightweight:** less resource consumption
Detection	-	-	R-CNN, Faster R-CNN, mask R-CNN, etc.	**Pros:** high detection accuracy
				Cons: slow detection speed
			YOLO, SSD, etc.	**Pros:** fast detection speed
				Cons: relatively low accuracy

losis bacilli, sperm shape, etc.) that are important for the detection of the characteristic disease (such as urinary tract infections, parasitic infections, tuberculosis infections, sperm abnormalities, etc.). The target cells in different specimens of natural exclusions are shown in Fig. 3. The application of AI techniques to the detection of target cells in different samples is described in detail below, and some of the latest advances are counted in Table 2.

Urine sample

In clinical practice, pathologists are often required to determine the physiological health of a patient by analyzing the

Fig. 3 | Target cells in different natural excrement samples. (**a**) Four different sperm head morphologies. (**b**) Images of sputum smears acquired under different microscopes. (**c**) Medically significant images of urine sediment. (**d**) Microscopic images of parasites in feces of medical significansce. Figure reproduced with permission from: (a) ref. [21], Elsevier; (b) ref. [22], IEEE Xplore; (c) ref. [23], IEEE Xplore; (d) ref. [24], Elsevier.

Table 2 | Application of artificial intelligence in natural shed cytology.

Sample	References	Task	Method	Accuracy (%)	Sensitivity (%)	Specificity (%)	Precision (%)	F1-score (%)	Data (images)
Urine	Ji et al[23].	Urine sediment	Classification: AlexNet, Area Feature Algorithm	96. 75	-	-	-	-	300,000
	Zhang et al[25].	Urine sediment	Classification: ResNet	97. 15	98. 73	95. 85	-	-	1,550
	Vaickus et al[26].	Urothelial carcinoma	Segmentation: VGG-19 Classification: AlexNet	95	-	-	-	-	-
	Nojima et al[27].	Suspicious atypical cells	Classification: VGG16	95. 36	90. 51	96. 82	89. 53	90. 02	466
	Tsuneki et al[28].	Urothelial carcinoma	Classification: ResNet-50, DenseNet-121, inception v3	94.6	96.0	94.6	-	-	786
	Wu et al[29].	Urothelial carcinoma	Detection: YOLOv7, efficientnet, convNeXt-B classification: attention-BiLSTM, Transformer, Top-N feature model	-	92.8	-	-	-	5260
	Naznine et al[30].	Urine sediment	Detection: YOLOv9e, KD-YOLOX-ViT Classification: YOLOv9e, KD-YOLOX-ViT	-	-	-	88.5%	-	5408
Fecal	Li et al[31].	Analysis of fecal composition	Classification: ResNet-152, FPN, FCN	-	93. 56	-	-	-	22,440
	Nkamgang et al[24].	Intestinal parasites	Segmentation: edge detector, hough transform Feature: HOG, LDA Classification: fuzzy neural network	100	-	-	-	-	1,240
	Tchinda et al[32].	Intestinal parasites	Segmentation: wavelet transform, etc Feature: PCA Classification: probabilistic neural network	100	-	-	-	-	900
	Yang et al[33].	SHT	Detection: ANN	-	82. 9	97. 1	-	-	2,078
	Dacal et al[34].	SHT	Detection: SSD Classification: MobileNet	-	80. 94	-	98. 44	88. 50	1,508
	Mathison et al[35].	Intestinal protozoa	Detection: CNN	-	-	-	-	-	-
	Lee et al[36].	Intestinal parasites	Segmentation: U-Net Detection: SSD, Faster R-CNN	-	-	-	-	-	-
	Tongjit et al[37].	Intestinal parasites	Detection: CNN	100	-	-	100	100	1250
	Soli et al[38].	Poultry fecal disease classification	Classification: HViT	90.9	89.43	-	89.43	88	6812
Sputum	Mithra and sam emmanuel[39]	Tuberculosis	Segmentation: multilevel thresholding Feature: LoH、SURF Classification: DBN	97. 55	97. 86	98. 23	-	-	275
	Chithra et al[40].	Tuberculosis	Segmentation: color space, adaptive thresholding Feature: color, texture, area, etc Classification: AFC-Deep CNN	93. 40	92. 60	-	-	-	75
	Hu et al[41].	Tuberculosis	Classification: inception v3	98. 4	98. 4	-	98. 4	98. 4	40
	Zachariou et al[42].	Tuberculosis	Synthesis: cycle-gan classification and Count: resnet, densenet, squeezenet	99. 74	96. 70	-	99. 00	96. 00	230
	Zachariou et al[43].	Tuberculosis	Segmentation: U-Net	-	-	-	-	-	1000
Sperm	Miahi et al[44].	Sperm morphology analysis	Classification: genas (proposed)	91. 66	95. 03	-	95. 40	-	1,540
	Abbasi et al[45].	Sperm morphology analysis	Classification: VGG19	94. 00	98. 09	-	95. 18	-	1,540
	Ilhan and Serbes[46]	Sperm morphology analysis	Classification: VGG16, googlenet	92. 13	-	-	-	-	1,132
	Zou et al[47].	Sperm detection	Detection: TOD-CNN(one-stage CNN model)	85. 60	89. 47		90. 00	90. 54	
	Yang et al[48].	Sperm Multidimensional morphology analysis	Classification: efficientnet Segmentation: segnet	90.82		-			30000-
	Turkoglu et al[49].	Sperm abnormality classification	Classification: deepmind's NFNet-F4,ViT	69.43/ 71.34/ 68.41	-	-	-	-	18462/ 18269/ 12631

microscopic analysis of tangible fractions in a urine sample. Certain deposits in urine can reflect the corresponding disease. Ji et al[23]. proposed a combined AlexNet and area feature algorithm (AFA) to detect urine sediment microscopic images, which solved the problem of CNN on weakening image features and achieved rapid identification of confusable objects of up to 10 types in urine sediment images. Zhang et al[25]. proposed a multi-view residual network-based cell recognition method for urine microscopic images, using multi-view residual networks to extract effective features of urine sediment from multiple perspectives to solve problems such as loss of cellular information.

Urine micrographs can also be used to detect urologic cancers. Vaickus et al[26]. proposed a combination of deep learning and morphological measurements to automate the Paris system. They proposed an algorithm called AutoParis, which intelligently analyzed cell morphology, classified different urine components, filtered invalid objects, and automatically generated tabulations of the Paris system criteria and a malignancy risk score. In particular, Nojima et al[27]. proposed a deep learning system trained with histological specimen information to assist in the detection of urothelial carcinoma (UC). The system can identify histological morphological features and use images of cytological specimens that support UC screening to determine whether the UC cells in the corresponding tissue specimens are high-grade or low-grade[27]. This can effectively help urologists screen for UC and plan treatment. Tsuneki et al[28]. are dedicated to alleviating the burden of pathologists searching through WSI. They employed transfer learning, fully supervised, and weakly supervised learning methods to train deep learning models, enabling the models to directly predict the malignancy of cells on WSI and highlight suspected tumor regions. Wu et al[29]. proposed an AI-based model called precision urine cytology AI solution (PUCAS) with multi-stage framework algorithms in a large, which helped to improve the sensitivity of urine cytology, reduce misdiagnoses of UC, avoid unnecessary endoscopy and reduce the clinical burden in resource-limited areas. They integrated three distinct feature extraction models (YOLOv7, EfficientNet, and ConvNeXt-B) and comprised three distinct models (the attention bi-directional long short-term memory, Transformer, and Top-N Feature model), enabling the models to simulate the consensus process of voting opinions of multiple experts[29]. More recently, Naznine et al[30]. proposed an ensemble framework that introduces a Vision Transformer (ViT) to urinary sediment detection. Their approach combines a CNN-based YOLOv9e model with a KD-YOLOX-ViT model, which integrates a ViT module to capture global contextual features beyond the capabilities of conventional CNNs. This ViT-enhanced ensemble, fused via Weighted Box Fusion, achieved a top mAP50 of 94.18% on the USE dataset and demonstrated strong generalizability (mAP50 94.64%) upon external validation, highlighting the value of Transformer architectures in advancing cytological image analysis.

Fecal sample

Cytological examination of feces can be used to diagnose diseases such as intestinal infections, parasitic infections, gastrointestinal bleeding, and inflammatory bowel disease. By observing the visible components in the microscope smear, such as parasite eggs, white blood cells, red blood cells, and intestinal mucosal epithelial cells, doctors can help determine the diagnosis and treatment plan for the disease. In fecal microscopic images, components such as parasitic eggs, white blood cells, red blood cells, and intestinal mucosal epithelial cells have received attention[31]. Many techniques based on image processing and machine learning have been proposed for the identification of organic matter content in feces[50–54]. Among them, Li et al[31]. proposed a network called FecalNet, which achieved over 90% recognition accuracy for various components by combining deep learning networks with multiple neural networks. Some studies have focused on the detection of parasitic eggs in feces. Methods based on fuzzy neural networks[24] and probabilistic neural networks[32] have been successively proposed, both achieving nearly perfect classification of parasites. Tongjit et al[37]. proposed a CNN for classifying and automatically detecting O.viverrini eggs, achieving a high detection accuracy.

Furthermore, in order to provide more efficient and accurate solutions, some researchers have begun to develop methods that integrate data collection or combine remote platforms to better integrate fecal automatic detection methods into clinical practice. Yang et al[33]. proposed a system called Kankanet, deployed through a smartphone application, for detecting the eggs of the three most common soil-transmitted worms in fecal samples. Dacal et al[34]. proposed a fully integrated telemedicine platform from fecal sample collection to automated sample analysis, as shown in Fig. 4(a,b), which accomplishes digitization and remote transmission of microscopic samples via smartphones and customized apps, and uses these data to train artificial intelligence models for automated detection and quantification of soil-transmitted helminths (STH). Mathison et al[35]. developed a sensitive CNN model, in conjunction with high-resolution digital slide scanning, for identifying and labeling intestinal protozoa in trichrome-stained human stool samples. Lee et al[36]. created a cloud-based platform integrating various deep learning strategies like Faster R-CNN, SSD, and U-net for intelligent analysis of worm eggs. As shown in Fig. 4(c,d), the platform allows users to analyze worm infections using multiple prediction options, perform fusion predictions based on aggregated results and allows users to upload their own datasets and predictive models for training and sharing. Notably, vision transformer (ViT) architectures have introduced new approaches to fecal image analysis. Soli et al[38]. developed a Hierarchical ViT (HViT) for poultry disease detection, which employs multi-scale

Fig. 4 | (**a**) Digitization solution for conventional microscope images, where the conventional microscope is connected to a smartphone via a 3D printing adapter. (**b**) Telemedicine web platform view for viewing and analyzing digitized samples for manual annotation. Web interface of HEAP: A user-friendly web system for uploading and processing cytological images, automatic detection and manual marking of parasites. (**c**) Lab management: create prediction. (**d**) List view: all candidate eggs. Figure reproduced with permission from: (a, b) ref. [34], PLOS; (c, d) ref. [36], Elsevier.

embedding and hierarchical attention to capture both local textures and global contexts in fecal images. On a dataset of 6,812 images, HViT achieved a 90.90% validation accuracy, outperforming standard ViT-B/16 and CNNs. It showed particular strength on the minority "newcastle" class, improving recall by 3.3%, demonstrating its utility in handling class-imbalanced cytological data.

Sputum sample

Cytological examination of sputum samples is typically used to investigate respiratory infections and inflammatory diseases. Currently, the most common application of artificial intelligence is for intelligent detection of Mycobacterium tuberculosis, there are two main ways to detect tuberculosis bacilli (TB), namely bright-field microscopy and fluorescence microscopy.

As shown in Fig. 4(b), under bright-field microscopy, TB is shown as purple or red with a blue background, while under fluorescence microscopy, the segmented TB is shown as green and yellow. The application of AI in bright-field microscopy images is first introduced. To address the shortcomings of traditional TB detection methods in terms of detection speed and response time, methods based on clustering[55], feature decomposition[56], random forest[57], and neural networks[58] have been developed.

To better detect the severity of sputum smear images and identify their infection levels, Mithra et al[39]. proposed a method combining multi-level threshold segmentation, feature extraction algorithms, and deep belief neural networks (DBN) for classification to accurately identify bacilli in sputum smear. In addition, Chithra et al[40]. designed an adaptive fractional crow (AFC)-deep CNN algorithm, which can detect the severity of images with a combination of features such as bacterial number, bacterial area, scattering coefficient, and skeleton features. To directly process WSI images, Hu et al[41]. proposed a method based on subgraph partitioning for automated detection and counting of tuberculosis bacilli.

Fluorescence microscopy images are more likely to distinguish mycobacterium tuberculosis from its surroundings than conventional microscopy[59]. Zachariou et al[42]. proposed a method for rapid detection and counting of mycobacterium tuberculosis using a cycle-consistent GAN to synthesize images, ultimately achieving a classification accuracy of 99. 74%. The following year, they also reported a method for localizing TB cells on stained fluorescence microscope images using U-Net[43].

Sperm sample

Cytological examination of semen is typically used for the investigation of male reproductive system-related diseases. Artificial intelligence methods have become another hot topic of research in the field due to their ability to exclude subjective factors and achieve more rapid sperm morphological analysis.

Ilhan et al[60]. proposed a computation framework including multi-stage cascade-connected preprocessing techniques, region-based descriptor features, and non-linear kernel SVM-based learning for the classification of stained sperm images. Respectively, this demonstrates that considering sperm orientation information in the images and employing effective noise cancellation techniques can improve classification accuracy.

Miahi et al[44]. proposed a neural architecture search algorithm called genetic neural architecture search (GeNAS) to predict the morphological defects in certain parts of the sperm and introduced a function called GeNAS weighting factor (GeNAS-WF) to evaluate the fitness of each structure. Its search process is shown in Fig. 5(a). The results demonstrate that the optimal neural structure discovered by GeNAS achieved satisfactory outcomes in detecting vacuolar anomalies. However, it is important to note that despite requiring less computational power and manpower compared to manually constructed structures or random search methods, the training of the network still took a considerable amount of time. Abbasi et al[45]. applied multi-task learning to sperm morphology analysis. They used a pre-trained network to perform multi-task learning on three labels in two stages, as shown in Fig. 5(b). In the first stage, the algorithm learned the common features of sperm images to improve prediction performance. In the second stage, each label was independently trained using the features obtained in the first stage, so that the network could classify the head, vacuole, and acrosome labels into normal or abnormal in a single prediction. To overcome the problems of image imbalance and low resolution in the dataset, Ilhan et al[46]. used an ensemble learning method. They fused the prediction results of different deep networks by soft voting and performed two-stage fine-tuning on multiple datasets to improve prediction accuracy. Yang et al[48]. developed a novel algorithm based on FairMOT, BlendMask, SegNet, and EfficientNet to enable non-invasive multidimensional morphological analysis of live sperm in motion, addressing the limitations of existing methods in accurately calculating minority groups of non-existent progressive motility and morphologically normal sperm. Turkoglu et al[49]. introduced a two-stage divide-and-ensemble framework to improve sperm morphology classification. They innovatively employed a vision transformer as a "splitter" to efficiently categorize sperm images into head/neck abnormalities versus tail abnormalities/normal, reducing inter-class confusion. An ensemble model integrating ViT and CNN architectures then performed fine-grained classification, aided by a multi-stage voting strategy for reliable decision-making. Achieving around 70% accuracy across datasets, their method significantly outperformed single-model baselines, underscoring the effectiveness of ViT in complex medical image analysis. In addition to this, many object detection models are used to detect sperm activity[47,61].

Summary

In the field of natural shed cytology, artificial intelligence has shown great potential in its integration with medical practice. For example, for urine specimens, methods that are beneficial to clinical testing have been developed that combine with specific systems[26] or with histological samples[27]. For stool specimens, methods that are beneficial to non-professionals have been developed that combine with medical internet and remote platforms[36]. For sputum specimens, data collection and infection recognition have been integrated with programmable microscopes[62]. For semen specimens, many sperm tracking technologies have been developed that can be used in clinical practice[47]. We also encourage more researchers in the field to focus on the research of artificial intelligence methods that benefit from interaction with multiple data sets and are applicable to multiple scenarios and to use advanced or traditional equipment combined with the internet to make artificial intelligence technology a "medical expert" that can serve everyone.

Body cavity effusion cytology

Body cavity effusion includes ascites, pleural effusion, and cerebrospinal fluid. The examination of body cavity effusion is helpful to the diagnosis of malignant tumor, and to trace the source and type of tumor, so as to provide the basis for clinical diagnosis[63]. The images of cytological specimens of body cavity effusion and the morphological representation of different cancer cells in it are shown in Fig. 6. This section details the specific application of AI methods to the examination of body cavity effusion samples and summarizes them in Table 3.

Pleural effusion sample

Cytological examination of pleural effusion is commonly used to detect malignant tumors within the pleural cavity, such as lung cancer, breast cancer, and mesothelioma. As the nucleus of a cancerous cell shows distinct morphological changes and abnormalities, segmenting the nucleus can help researchers to quickly locate the cancerous cells. At present, only a small number of literature has studied the application of deep learning in the diagnosis of pleural cancer. Detectors such as SSD, Faster R-CNN, and R-FCN have been used for nucleus detection in pathological images[66]. FCN, SegNet, and U-Net have been used for pleural nucleus segmentation[63].

Furthermore, in order to validate the significant potential of artificial intelligence technology in addressing the scarcity of expert resources, Xie et al[67]. proposed a weakly super-

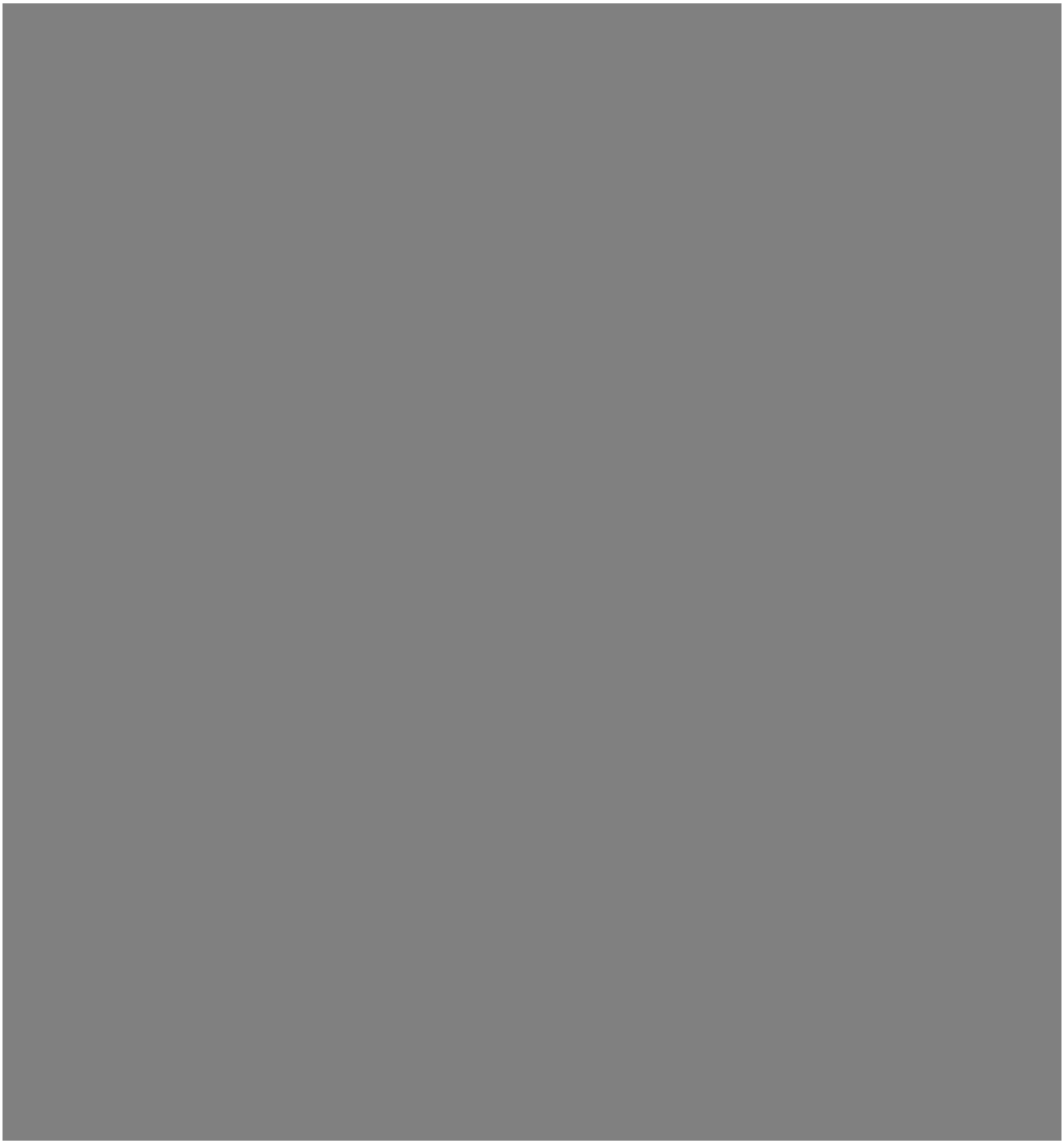

Fig. 5 | (**a**) Overall scheme diagram of NAS algorithm. (**b**) Deep multi-task transfer learning (DMTL) model. The model was used to extract effective features shared by the three tasks and an output layer with a vector of three elements was designed to represent the probability of anomalies for each of the specific sections. Figure reproduced with permission from: ref.[44], Elsevier; ref.[45], Elsevier.

vised method based on multiple instance learning (MIL) for WSI classification. They utilized a ResNet-18 network to build a classifier for distinguishing benign and malignant cells in cytological images and analyzed pleural effusion images. Similarly, using the MIL approach, Ren et al[68]. not only focused on the benign and malignant diagnosis of pleural effusion but also employed artificial intelligence techniques to identify the primary sites of common metastatic cancers in pleural effusion and predict genetic changes related to targeted therapy, assisting medical experts in more precise drug treatments. Tian et al[69]. proposed the Ultra-Multi-SWIN model, which introduces a multi-directional-shift window attention mechanism to focus on key features at effusion boundaries and uses a masking module to suppress irrelevant information. This design integrates physician diagnostic experience as inductive biases, enabling

Fig. 6 | (**a**) An example of a stained body cavity effusion cytological image. (**b**) Morphology of different types of normal and cancerous cells in images of body cavity effusion specimens. Figure reproduced with permission from: ref.[64], IEEE Xplore; ref. [65], Frontiers.

Table 3 | Application of artificial intelligence in body cavity effusion cytology.

Sample	References	Task	Method	Accuracy (%)	Sensitivity(%)	Specificity(%)	Precision (%)	mAP (%)	Data (images)
Pleural effusion	Xie et al[67].	Cancer cells classification	Classification: ResNet-18	91. 67	87. 50	94. 44			404
	Ren et al[68].	Cancer cells classification	Classification: inception-ResNet-v2	89.1	91.1	87.0		90.9	1321
	Tian et al[69].	Pleural effusion severity classification	Classification: ultra-multi-swIN	98.8/95.2	-	-	-	-	25442
Ascites	Su et al[70].	Peritoneal metastasis	Detection: faster R-CNN Classification: alexnet, VGG16, googlenet, ResNet-18, ResNet-50				96. 80		663
	Kim et al[71].	Metastatic colorectal cancer	Classification: Mobilenet-v2, xception	93.74	87.76	87.76			70,162 (patchs)
	Tian et al[72].	Cancer of unknown primary	-	82.6					57,220 (patchs)
Cerebrospinal fluid	Yu et al[65].	CSF cells classification	Detection: faster R-CNN					95	53,255
	Schweizer et al[73].	CSF cells classification	Classification: VGG-16						123,181
	Zhang et al[74].	DL-SERS classification	Classification: transformer	96.13	-	-	-	-	12319

strong generalization with limited data. It achieved a high accuracy of 0.952 (subject-independent) on a 50-subject dataset, demonstrating its potential for application in portable ultrasound devices.

Ascites sample

Cytological examination of ascitic fluid is routinely employed to detect malignant tumors within the peritoneal cavity, including those originating from ovarian, gastric, pancreatic, and colorectal origins. To swiftly ascertain whether ascites is cancer-induced, Su et al[70]. introduced an end-to-end deep learning system tailored for automated interpretation of ascitic cytology. This system efficiently localizes cells followed by the deployment of multiple classification models to achieve precise differentiation between benign and malignant cells, integrating detection and classification networks for accurate assessment of peritoneal metastasis status. Meanwhile, Kim et al[71]. have concentrated on enhancing the accuracy and sensitivity of pathologists' diagnosis of metastatic colorectal cancer (CRC) through the employment of AI technologies. Of particular note, given the challenge posed by patients with carcinomas of unknown primary (CUP) presenting with pleural or peritoneal metastases, Tian et al[72]. have devised a deep learning methodology utilizing cytological histology for tumor origin discrimination. This innovation not only identifies malignancy but also predicts the origin of tumors in pleural effusions and ascitic fluids.

Cerebrospinal fluid sample

Cerebrospinal fluid (CSF) cytology is frequently employed in the detection of malignant tumor cells within the CSF, such as those associated with meningiomas, intraventricular tumors, and leptomeningeal metastases (LM). Yu et al[65]. introduced two convolutional neural network (CNN) approaches, separately tailored for the detection of intracranial and extracranial tumors. Given the difficulty in subclassifying cancer cell subtypes based solely on morphological characteristics, they integrated patient medical history and auxiliary examinations to attain precise cancer annotations,

thereby enhancing the predictive accuracy of their model. Subsequently, addressing more intricate diagnostic challenges, Schweizer et al[73]. proposed a deep learning methodology capable of identifying 15 diagnostically relevant cell types in CSF, and leveraged layer-wise relevance propagation (LRP) for computing feature heatmaps, thus augmenting the interpretability of their CNN model. These studies collectively emphasize that AI methodologies can significantly reduce the workload and time required by medical professionals for diagnosis. Zhang et al[74]. proposed an innovative deep learning-assisted SERS (DL-SERS) framework. Its core innovation lies in the fusion of 1D spectral and 2D image features, coupled with a Transformer model for learning and classification. This technology requires only 0.5 μL of CSF to achieve accurate diagnosis of acute leukemia subtypes, genetic abnormalities, and central nervous system involvement within 5 minutes, with an accuracy exceeding 90%, demonstrating the great potential of advanced models in molecular diagnostics of cerebrospinal fluid.

Fig. 7 | Examples of benign cells (left) versus malignant cells (right) in FNAC cytological images of different specimens. Figure reproduced with permission from ref. [79,81,101–103], Springer Nature, Elsevier, Wiley-Blackwell, MDPI.

Summary

Overall, the application of artificial intelligence technology in body cavity effusion cytology is currently insufficient, and there is a lack of publicly available and widely recognized datasets in this field. However, existing research has demonstrated that artificial intelligence technology has great potential in the rapid localization and identification of cancer cells in body cavity effusion. Therefore, we encourage more researchers to explore the research value of this field.

Fine needle aspiration cytology

Fine needle aspiration cytology (FNAC) can be used to make a conclusive diagnosis of cancer, in which a narrow bore needle is used to collect a tissue lesion sample for microscopic examination. Compared to histopathology, FNAC is minimally invasive and can accomplish a rapid diagnosis and shorten or avoid hospitalization. Images of a common FNAC specimen are shown in Fig. 7. An increasing number of CADs are now beginning to utilize artificial intelligence to accomplish the automation of diagnosis[100]. This section will detail the use of artificial intelligence techniques in FNAC slice analysis and the corresponding cancer-assisted diagnosis and show the important details in Tab. 4.

Breast sample

Breast FNAC can assist physicians in diagnosing the nature of breast masses, including benign tumors, malignant tumors, or other lesions. If cancer cells are identified in the breast FNAC sample, physicians can further determine the type, grade, and treatment plan for the cancer. Some researchers focus on using artificial intelligence for early screening of breast cancer, with their main goal being the binary classification of benign cells and malignant tumor cells. For example, Khan et al[104]. proposed a framework that combines machine learning and computational intelligence in electronic healthcare services to achieve remote early detection and classification of malignant breast cancer cells. They improved classification accuracy by optimizing morphological feature extraction and utilized three commonly used algorithms for binary classification of tumor cells into benign and malignant categories.

Saikia et al[75]. and Miselis et al[76]. have demonstrated through a comparison of various deep learning methods that the Inception v3 network exhibits excellent performance in benign and malignant diagnosis of breast FNAC cell samples. Zerouaoui et al[77]. combined seven DL techniques for feature extraction and four classifiers for binary classification of breast cytological images on the FNAC dataset, and the validation showed that a hybrid architecture using DenseNet201 for feature extraction and MLP as a classifier achieved the best performance with 99% accuracy. To reduce the time spent in region of interest (ROI) detection, Bal et al[78]. used the YOLO v3 network as a region proposal network (RPN) to achieve automatic ROI detection and applied the extracted ROI patches to the classification training of the CNN model. The validation showed that the highest accuracy with YOLO v3 was 98.9%. In order to make artificial intelligence models more concise and suitable for breast cancer detection, Bal et al[79]. developed a novel CNN network called BFCNet and created a new breast lesion FNAC image dataset. Experimental results have shown that their approach surpasses five other common networks, achieving an average accuracy of 97.81%. Zhao et al[105]. proposed a weakly-supervised Label-Efficient WSI Screening method, dubbed LESS, designed to learn reliable patch features, even from small datasets. In breast imaging analysis, Abdallah et al[80]. proposed the PatchCascade-ViT framework that innovatively applies self-supervised vision trans-

Table 4 | Application of artificial intelligence in Fine needle aspiration cytology.

Sample	References	Task	Method	Accuracy (%)	Sensitivity(%)	Specificity(%)	F1-score (%)	Data (images)
Breast FNAC	Saikia et al[75].	Breast cancer	Segmentation: otsu thresholding Classification: inception v3, VGG16, VGG19, ResNet-50	96. 25				212
	Miselis et al[76].	Breast cancer	Classification: alexnet, googlenet, squeezenet, densenet, inception v3	91. 86				67
	Zerouaoui et al[77].	Breast cancer	Classification: ensemble learning, MLP, DenseNet-201, Inception-v3, ResNet-50, MobileNet-v2, VGG16, SVM, DT, KNN, etc	99. 00	98. 49		99. 02	212
	Bal et al.2021b[78]	Breast cancer	Detection: YOLO-v3 Classification: VGG16, ResNet-50, Inception-v3	98. 9	98. 2	100		135
	Bal et al.2021a[79]	Breast cancer	Classification: bfcnet(proposed)	97. 81	97. 3	98. 2	97. 5	1,651
	Abdallah et al[80].	Breast cancer	Classification: patchcascade-ViT	-	85.01	-	84.9	12476
Thyroid FNAC	Sanyal et al[81].	PTC	Classification: CNN	85. 06	90. 48	83. 33		370
	Guan et al[82].	PTC	Classification: VGG-16, inception-v3	97. 66	100	94. 91		887
	Duc et al[83].	PTC	Classification: ensemble learning, resnet, densenet, inception-v3, SVM, KNN, adaboost	99. 71				367
	Zhang et al[84].	Thyroid cancer	Classification: transformer	94.87	-	-	-	22111
Lung FNAC	Tsukamoto et al[85].	Lung cancer	Classification: AlexNet, GoogLeNet, VGG16, ResNet-50, NB, SVM, RF, NN	78. 9				298
	Teramoto et al[86].	Lung cancer	Classification: ad mil, alexnet	91. 6	93. 0	88. 9		3,057
	Ai et al[87].	Lung cancer(ROSE)	Classification: densenet-169	84. 57				627
	Lin et al[88].	Lung cancer(ROSE)	Segmentation: hrnet Classification: ResNet-101	98. 8	98. 8	98. 8		499
Pancreatic FNAC	Boroujeni et al[89].	Pancreatic cancer(ROSE)	Segmentation: k-means clustering Feature: shape Classification: MNN	100				277
	Zhang et al[90].	Pancreatic cancer(ROSE)	Segmentation: U-Net Classification: ResNet-101	95. 8	94. 4	97. 1		5,345

formers (ViTs) to BI-RADS classification of mammograms. Through self patch-level supervision pre-training, the ViT learns effective features from unlabeled data, significantly reducing annotation dependency. Its two-stage cascade classification enables precise diagnosis from initial cancer screening to tissue density subtyping, achieving 85.01% sensitivity and 84.90% F1-score on 4,368 cases and outperforming traditional CNN models.

Thyroid sample

Thyroid FNAC is primarily used to evaluate the benign or malignant nature of thyroid nodules. To automate the cytological examination of thyroid nodules, some scholars have proposed models combining classifiers, such as SVM and various morphological features[106,107], recognition models based on super-pixel segmentation[108], and multi-instance weakly supervised machine learning models.

In order to distinguish papillary thyroid carcinoma (PTC) from non-PTC in microscopic images, Sanyal et al[81]. developed a CNN, which has a sensitivity of up to 90. 48%. However, the method did not achieve high accuracy due to the misidentification of faint papillary structures formed by benign follicular cells as papillary carcinoma. To address this problem, Guan et al[82]. proposed a deep network based on VGG-16 and Inceptionv3 to identify PTC tissue from cell sections. They quantified the morphological features of tumor cell nuclei as the average of contour, perimeter, area, and pixel intensity.

The above methods process patches rather than whole FNAC images, and the detection of whole FNAC smears is more suitable for use in clinical care. To bridge this gap and provide an end-to-end complete automated diagnostic system, Duc et al[83]. proposed an integrated deep learning framework that combines the prediction of multiple individual deep learning models, including ResNet, DenseNet, and Inception to efficiently and automatically extract cytological features from PTC smears, and uses several traditional supervised machine learning algorithms such as SVM and AdaBoost to achieve the final prediction as a way to improve detection accuracy. The validation showed that combining multiple CNN models with AdaBoost classifiers achieved the best prediction performance, reaching a

high accuracy of 99.71%. Zhang et al[84]. introduced multi-dimensional knowledge distillation to compress a 12-layer ViT teacher model into a 3-layer ViT student model. Trained on 22,111 thyroid cytopathological patches, the student model achieved a Top-1 accuracy of 94.87%—only 0.55% lower than the teacher—while reducing computational complexity by approximately four times, offering an efficient and accurate solution for clinical thyroid nodule diagnosis.

Lung sample

Lung FNAC is commonly used for lung cancer detection. Tsukamoto et al[85]. compared the prediction performance of four fine-tuned DCNN models in lung cancer cytological image classification. To classify normal and malignant lung cells more precisely, they use generative adversarial networks (GAN)[109] to automatically generate cytological images. They confirmed that GAN networks were effective in helping cytological images to complete classification with limited data.

Since labeling all cells in the supervised learning approach is a big challenge, Teramoto et al[86]. developed another weakly supervised classification method based on attention-based deep multi-instance learning (AD MIL) to automatically classify benign and malignant lung cells without complex annotations, achieving a better classification correct rate of 91.6% compared to supervised learning. Ai et al[87]., on the other hand, proposed a CNN model based on DenseNet-169, and they also compared the classification results of the AI with those of pathologists, and their results showed that the accuracy of the method was not significantly different from that of primary pathologists. To further improve the classification accuracy, Lin et al[88]. combined deep learning classification of lung cytological images with semantic segmentation and proposed a ResNet-101-based method to distinguish benign and malignant lung cells, and achieved a classification accuracy of 98.8%. Sun et al[110]. pioneered the use of a hierarchical Swin Transformer with shifted windows for lung CT analysis. This architecture efficiently captured features at multiple scales, achieving superior performance in both lung nodule classification and segmentation tasks compared to standard ViT and CNNs.

Pancreas sample

Artificial intelligence has been less applied in rapid on-site cytopathology evaluation (ROSE) of endoscopic ultrasound-guided fine-needle aspiration (EUS-FNA) of the pancreas. In the conference abstract, Thosani et al[111]. presented a preliminary diagnosis of EUS-FNA cytopathology images using an artificial intelligence approach to complete An in-depth study of the interpretation was carried out. Boroujeni et al[89]. proposed a multilayer perceptron neural network (MNN) for differentiating benign and malignant cases of pancreatic cancer. The method achieved 100% accuracy in the classification of benign and malignant and also had some predictive power for atypical data sets. Most notably, Zhang et al[90]. proposed a DCNN-based segmentation model, which was constructed based on ResNet-101, whose main work was to distinguish stained cells from the background and identify pancreatic malignant cell clusters in cytopathological sections. In particular, they used an adequate internal and external dataset to validate the recognition effectiveness of the DCNN system, demonstrating that the method can reach the level of cytopathologists in terms of detection accuracy and has good potential for application.

Summary

In many studies of fine needle aspiration cytology, researchers compare multiple deep learning networks to select the one that performs better. In deep learning, feature extraction is very abstract, and performance is greatly affected by hyperparameter selection. Therefore, it is difficult for researchers to directly discover networks with obvious advantages. However, selecting a network based solely on simple performance comparison lacks interpretability. It is better to understand the principles involved through model distillation or intermediate layer visualization. In addition, some researchers choose to create specialized recognition networks for specific cytological images[79]. We also encourage researchers to combine domain-specific expertise with advanced network structures and ideas to create emerging networks rooted in the cytology field.

Other cytology

In addition to the above samples, there are a number of cytological samples that are also important in clinical diagnosis, such as cytological specimens of the endocervix, which are used as important indicators to screen for cervical cancer, and AI-based methods have also received a lot of attention in this field[112,113]. The images of typical cervical cytology specimens is shown in Fig. 8. This section will detail the specific application of AI methods to other samples represented by cervical cytology, with important details in Table 5.

Fig. 8 | Examples of different grades of cervical cytological images using TBS as a standard. Atypical squamous cells of undetermined significance (ASC-US) on the left and high-grade SIL (HSIL) on the right. Figure reproduced with permission from ref. [114], Karger.

Table 5 | Application of artificial intelligence in scraping cytology.

Sample	References	Task	Method	Accuracy (%)	Sensitivity(%)	Specificity(%)	F1-score(%)	Data(images)
Endometrial	Hussain et al[91].	Cervical cancer	Classification: ensemble learning, AlexNet, VGG16, VGG19, ResNet50, ResNet101, GoogleNet	98. 9	97. 8	97. 9		1670
	R. Wang et al[92].	Cervical cancer	Classification: ResNet50, DenseNet121	96. 33				5015
	Gao et al[93].	Cervical cancer	Classification: ResNet50	98. 52	98. 53	98. 68	98. 59	5015
	Rahaman et al[94].	Cervical cancer	Classification: feature fusion, VGG16, VGG19, xception, ResNet50	99. 14	99. 0		99. 0	4049
	Ghoneim et al[95].	Cervical cancer	Classification: VGG16, CaffeNet, extreme learning machine	97. 2				917
	Zhu et al[96].	Cervical cancer	Segmentation: U-Net Detection: YOLO-v3 Classification: xception, xgboost, decision tree		92. 00	82. 14		81,727 (samples)
	Cheng et al[97].	Cervical cancer	Classification: ResNet50, densenet		95. 1	93. 5		3,545
	Zhang et al[98].	Cervical cancer	Classification: ResNet50, ResNet101, PVT, swin transformer					3092
	Nirmala et al[99].	Cervical cancer	Classification: CNN, AVTE, ADRAN	-	-	-	-	917

Cervical sample

Similar to breast cancer, cervical cancer is also a common cancer among women, with hundreds of thousands of women dying from it globally each year. Regular check-ups are an effective method for preventing cervical cancer. To assist doctors in speeding up screening and improving detection accuracy, AI-based automated cancer cell recognition methods have been developed with high expectations. Many researchers have validated the feasibility of using AI to assist with cervical cytology[115–117].

Researchers have successfully applied an integrated deep learning model based on decision fusion[91], attention-based frameworks[92], and knowledge distillation[93] techniques to improve the classification of cervical cytology. Specifically, decision fusion integrates the outputs of multiple models to achieve more robust and consistent predictions; attention-based frameworks enable models to focus on the most informative cellular regions for feature extraction; and knowledge distillation transfers knowledge from a complex teacher network to a simpler student network to enhance learning efficiency. While a combination of deep learning methods and an extreme learning machine has achieved high accuracy in seven-level classification[95]. These advancements highlight the effective utilization of AI-based methods in improving the prediction quality and generalization ability of cervical cytology classification.

In order to achieve more intelligent, refined, and clinically guided hierarchical management of cervical lesion risks compared to the five-level classification, Zhu et al[96]. proposed a cervical cytology grading diagnostic system based on TBS standards[114]. The system integrates single-class YOLOv3 for rapid semi-supervised annotation, multi-class YOLOv3 for detecting lesion cells, Xception for promoting lesion classification, Patch model for improving recognition accuracy, U-net for cell nucleus segmentation, and XGBoost model and logical decision trees for predicting the final TBS classification.

Meanwhile a progressive lesion cell recognition method that combines low-resolution and high-resolution WSI was proposed by Cheng et al[97].. The method consists of three parts: LR model for locating suspicious areas, HR model for recognizing lesion cell probability in patches, and WSI classification model for lesion classification. With a large dataset, effective data augmentation, diverse learning, and hard sample mining strategy, their system achieved high specificity, fast recognition of gigapixel WSI, and demonstrated advantages over existing commercial systems.

Moreover, Zhang et al[98]. proposed a novel semi-supervised learning framework SCAC, which addressed the challenge of limited labeled data in deep learning-based cervical abnormal cell detection and created the first large-scale publicly available unlabeled dataset. In SCAC, they introduced an advanced transformer module to mimic pathologists in conducting global comparisons and proposed a global attention feature pyramid network (GAFPN), which enhances multi-scale feature extraction by integrating high- and low-level features through an attention-based fusion mechanism, thereby improving the detection of both small isolated cells and large clustered abnormalities. In terms of innovation in model architecture and optimization strategies, researchers are also exploring cutting-edge technologies. Nirmala et al[99]. proposed an automatic cervical cancer classification system combining an adaptive vision transformer encoder with a convolutional neural network. The system performs precise cell segmentation via an adaptive deep residual aggregation network and utilizes an adaptive cat swarm optimization algorithm to automatically tune the key hyperparameters of the trans-

former, achieving an impressive accuracy of 97.43% on a seven-class cervical cell classification task. This work demonstrates the significant potential of integrating advanced transformer architectures with intelligent optimization algorithms to enhance the performance of complex medical image classification models.

Summary

In other cytology, such as cervical cytology, AI methods have shown remarkable success in saving time and improving screening efficiency in cytology. Researchers are actively developing more refined AI methods in line with clinical grading guidelines. The availability of large, diverse datasets greatly influences the credibility and practical value of these algorithms. Therefore, it is encouraged for researchers to propose or utilize large-scale public datasets, ensuring privacy and security through methods like federated learning.

Precise identification of WSI poses a challenge due to their size. Directly applying deep learning networks to process these ultra-large images is currently difficult. Hence, exploring the combination of WSI with patches, as demonstrated by Cheng et al[97]., is a promising direction. Further interesting solutions in this area are eagerly anticipated.

Challenges and conclusion

In the preceding section, it was observed that AI has been extensively employed across diverse domains of cell image analysis and has unequivocally exhibited its potential. However, in tandem with its potential, it confronts significant challenges in the areas of data, method selection, and practical applicability. Therefore, as shown in Fig. 9, this section aims to present promising solutions to these pervasive challenges and offer insightful support for the emergence of advanced research.

Dataset related

Dataset scarcity issues and solution

The lack of publicly available datasets and annotations in cytology processing has been a problem[118]. Transfer learning and data augmentation are common solutions to overcome data scarcity. Transfer learning utilizes data from related domains to identify salient features faster[119], while data augmentation techniques like cropping, rotation, and brightness adjustment improve model generalization. Another approach is to use generative models like GANs to synthesize high-quality data examples. However, stable GAN network training remains a challenge in creating synthetic cytological datasets[42,109].

Dataset imbalance issues and solution

Imbalance in cytological image datasets is a common problem, leading to incorrect classification and degraded prediction performance. Category imbalance in classification arises from the variation in the number of different cells, while in detection, it arises from a large number of candidate regions but only a few containing objects of interest[120]. Transfer learning and data augmentation methods can partially alleviate dataset imbalance. Other feasible solutions include resampling techniques to balance the dataset and custom loss functions to reduce the weight of simple negative samples during training. For example, Miahi et al[44].

Fig. 9 | Advantages and disadvantages of cytology image analysis methods based on artificial intelligence and promising methods.

proposed a custom loss function called GeNAS-WF to address dataset shortage and category imbalance.

High resolution global image detection solution

The development of WSI has allowed for the rapid generation of large 2D images in cytology, which provides physicians with a broader view for better application in actual clinical care[121,122]. However, detecting target objects in these images presents a challenge due to the large image size and small cell sizes. Two proposed solutions are the subgraph-based segmentation strategy and the open-source software-based segmentation strategy. The subgraph-based approach involves uniformly partitioning the WSI into subgraphs for annotation and detection[41,123]. Fast localization of target regions using object detection techniques is also a reliable method[96]. In addition to this, open-source software like QuPath[124] provides a scalable and user-friendly solution, allowing for hierarchical and object-based data modeling, interactive annotation, and automatic segmentation. These strategies have shown promising applications in cytological image analysis.

Method selection related

Method selection at the data label level

Cytological image analysis tasks can be classified into supervised and unsupervised learning. Supervised learning methods have been successful but require time-consuming and labor-intensive data annotation. Unsupervised learning lacks a clear objective function, making it challenging to evaluate model performance. However, recent research on unsupervised domain adaptation shows promise in improving model performance without additional target domain labeling[125]. This method transfers knowledge from a labeled source domain to the target domain. Combining this method with federated learning can address the challenge of utilizing private medical datasets and reduce the burden of data labeling.

Methods bridging supervised and unsupervised learning are also emerging to address undertrained models due to a lack of data labels. Weakly supervised learning in cytological images involves mapping input data to stronger labels using algorithms trained on known data and weak labels. One of the most commonly used when analyzing cytological images is MIL[67,86], where complete microscopic images are treated as bags and image patches as instances. MIL allows for classification based on bags, accommodating incorrect instances. Semi-supervised learning addresses the scarcity of labeled data by utilizing a large amount of unlabeled data to improve classification performance[126,127]. Semi-supervised learning models include self-training, co-training, multi-view training, etc. Among them, multi-view training has been successfully applied in the field of cytological images[128]. Self-supervised learning, designed for unlabeled datasets, enhances feature extraction by creating proxy tasks based on the data's representational properties, which has been successfully applied to cytological image segmentation[129].

Method selection based on model or task integration

Model or task integration is another approach to improve performance in intelligent image analysis tasks. Ensemble learning, which combines separate models, can significantly reduce prediction variance and improve results in cytological image analysis[130], a fusion method often used is decision-level fusion[46,86]. MIL is likewise a fusion method that exploits knowledge interactions between different views and performs data fusion during model design. It is beneficial when the underlying learner is not competent. Multi-task learning exploits similarities between different tasks and combines solutions in a single model, obtaining more integrated and meaningful information from the data[131], which has now been successfully used in the detection of sperm abnormalities[45].

Method selection for targeted model design

Most of the current models in cytological image analysis are obtained by retraining based on existing neural network structures. Most of these neural network structures are proposed to solve other problems, they are either very wide or very deep, and although they achieve good prediction results by transfer learning, they lack relevance to specific cytological samples. To obtain network structures that are more suitable for cytology, some experts choose to design networks manually. For example, BFCNet[79] and AFC-DeepCNN[40] have been proposed for breast sample and sputum sample analysis, respectively. The second approach is neural architecture search (NAS), which automates the design process and maximizes performance by proposing suitable models based on the given task and dataset[132].

Better clinical practice related

Combined mobile scanning and telemedicine system

practical and scalable cloud platforms for cytological image analysis has been developed in recent years. Through the cloud platform, remotely acquired images can be transferred from smartphones to telemedicine platforms via mobile networks for visualization, management, and labeling. Standard clinical and analytical procedures are transformed into digital tasks on the cloud platform. All acquired images can be annotated by specialists using the telemedicine platform, and the annotated data can be accessed by other experts to aid in diagnosis.

Remote platform based technologies are now well used for parasite detection in fecal samples, some of them are dedicated to providing accessible healthcare services in remote areas[33] and others are dedicated to provide more user friendly platform services[36]. The integration of intelligent

detection, mobile acquisition, and remote telemedicine systems often demonstrates superior potential in medical practice. It is encouraged that researchers, based on practical considerations, develop more open and practical remote platforms to enhance the interactive exchange of cytological image information.

Combined other detection methods

With the increasing maturity of various detection technologies, biomedicine is in a data revolution. Nowadays, extensive clinical data sets can be obtained, including complete high-resolution imaging, electronic medical records, human genome, etc[133].. This allows the analysis of diseases to be no longer limited to a single sample. At present, methods have been proposed to combine the detection result of cytological samples with that of histological analysis to obtain more reasonable diagnostic results[27]. Besides, when it is difficult to make the pathological diagnosis through morphology, patient history, neuroimaging, immunohistochemistry and other auxiliary detection can also be used to obtain a more accurate judgment[65]. At present, most studies focus on single or multiple data sets of the same type, but with the maturity of the scalable medical cloud platform, a comprehensive pathological diagnosis platform that integrates multiple types of medical information may become a promising research direction.

AI misuse, risks, and governance

Artificial intelligence has greatly advanced cytological image analysis, but its rapid adoption also brings potential risks that must be carefully managed before clinical deployment. Despite high reported accuracy in experimental evaluations, AI systems can sometimes fail in real-world scenarios due to shortcut learning, data leakage, or acquisition bias. Shortcut learning occurs when a model relies on spurious correlations —such as background color or imaging artifacts—rather than true cytomorphological features, leading to unreliable predictions. Similarly, hidden data overlaps between training and testing sets or biases introduced by single-center data collection can result in overestimated model performance.

Another emerging concern lies in the use of virtual staining and generative pipelines. While such techniques can enhance image visualization, they may also produce artifacts or hallucinated features that mislead diagnostic interpretation[134]. Therefore, integrating quality control mechanisms, including artifact detection, standardized imaging protocols, and model validation on raw clinical data, is crucial to prevent clinical misjudgment.

Ensuring model robustness and reliability further requires the incorporation of uncertainty estimation and out-of-distribution (OOD) detection. These mechanisms allow models to quantify confidence levels and identify unfamiliar input conditions, enabling clinicians to make informed decisions rather than relying solely on automated outputs.

Beyond algorithmic reliability, data privacy and governance represent another critical aspect. Cytological image data are not inherently difficult to obtain, but large-scale dataset construction remains challenging due to patient privacy and security concerns. Medical image data are typically stored in isolated institutional databases, making centralized aggregation impractical. To address this issue, Federated Learning(FL)[120] has emerged as a promising privacy-preserving paradigm that enables distributed training across multiple medical centers without exchanging raw patient data. By sharing only model parameters or gradients, FL effectively mitigates confidentiality risks. Although still facing challenges such as communication overhead and data heterogeneity, FL holds substantial potential for promoting collaborative yet privacy-compliant AI development in cytology.

In summary, responsible AI deployment in cytological image analysis requires a holistic governance framework that encompasses technical robustness, interpretability, data privacy, and ethical accountability. Continuous validation, transparent uncertainty reporting, and regulatory oversight will be essential to ensure that AI systems become not only accurate but also trustworthy and safe for clinical practice.

Conclusion and outlooking

This study reviews the latest advances in optical sensing, summarizing the most representative technologies in the field, including bright-field microscopy, fluorescence microscopy, and super-resolution microscopy. It also presents recent progress in AI-based cytological image analysis, covering key methods such as feature extraction, image segmentation, object detection, and image classification. In addition, this review discusses the structural and performance differences among various models and highlights promising techniques —such as attention mechanisms, ensemble learning, multi-task learning, multi-instance learning, and neural architecture search —that can help improve analytical performance and guide researchers in model selection. Furthermore, it provides a comprehensive summary of automated cytological image analysis applications in detecting different diseases, illustrating the uneven development of AI in analyzing diverse cytological samples and offering valuable references for future applications.

Looking ahead, we encourage researchers to focus on emerging AI technologies and to flexibly integrate the strengths of various methods. By combining the aforementioned optimization strategies with cytological expertise, it is possible to develop disease detection models with higher predictive accuracy and to establish cloud-based diagnostic platforms with better practical applicability. These efforts will help advance intelligent cytological analysis toward more accurate, efficient, and accessible healthcare solutions.

References

1. Schwab M. *Encyclopedia of Cancer* 3rd ed (Springer, Berlin Heidelberg, 2011).
2. Ivanovic M. Overview of cytopathology procedures and techniques. In Nayar R. *Cytopathology in Oncology* 1–12 (Springer, Berlin, Heidelberg, 2014); http://doi.org/10.1007/978-3-642-38850-7_1.
3. Jing X. Body cavity effusions and washings. In Xu HH, Qian XH, Wang H. *Practical Cytopathology: Frequently Asked Questions* 127–142 (Springer, Cham, 2020); http://doi.org/10.1007/978-3-030-24059-2_9.
4. Matias AV, Amorim JGA, Buschetto Macarini LA, Cerentini A, Casimiro Onofre AS et al. What is the state of the art of computer vision-assisted cytology? A Systematic Literature Review. *Comput Med Imaging Graphics* **91**, 101934 (2021);
5. Ma X, Zhang ZB, Yao MH, Peng JZ, Zhong JG. Spatially-incoherent annular illumination microscopy for bright-field optical sectioning. *Ultramicroscopy* **195**, 74–84 (2018);
6. Gutiérrez-Medina B. Optical sectioning of unlabeled samples using bright-field microscopy. *Proc Natl Acad Sci USA* **119**, e2122937119 (2022);
7. Chen ZY, Mc Larney B, Rebling J, Deán-Ben XL, Zhou QY et al. High-speed large-field multifocal illumination fluorescence microscopy. *Laser Photonics Rev* **14**, 1900070 (2020);
8. Zhang HY, Hu YT, Pu XW, Zhang SZ, He Y et al. LED-based multicolor extended resolution transmission fluorescence microscopy. *J Biomed Opt* **30**, 046501 (2025);
9. Kim GH, Chung J, Park H, Kim D. Single-molecule sensing by grating-based spectrally resolved super-resolution microscopy. *Bull Korean Chem Soc* **42**, 270–278 (2021);
10. Toy MF. Wedge prism assisted quantitative phase imaging on standard microscopes. *Opt Commun* **451**, 361–366 (2019);
11. Sun JW, Zhao B, Wang D, Wang ZG, Zhang J et al. Calibration-free quantitative phase imaging in multi-core fiber endoscopes using end-to-end deep learning. *Opt Lett* **49**, 342–345 (2024);
12. Li ZM, Costa PC, Guang Z, Serafini CE, Robles FE. GAN-based quantitative oblique back-illumination microscopy enables computationally efficient epi-mode refractive index tomography. *Biomed Opt Express* **15**, 4764–4774 (2024);
13. Shen CY, Li JX, Mengu D, Ozcan A. Multispectral quantitative phase imaging using a diffractive optical network. *Adv Intell Syst* **5**, 2300300 (2023);
14. Gu YF, Liu TZ, Gao GM, Ren GB, Ma Y et al. Multimodal hyperspectral remote sensing: an overview and perspective. *Sci China Inf Sci* **64**, 121301 (2021);
15. Jiao CW, Chen ML, Li ZH, Chen JB, Liao JQ et al. Lymph node diagnosis for colorectal cancer by utilizing a hyperspectral laparoscope and machine learning. *Prog Electromagn Res Pier* **182**, 55–61 (2025);
16. Yang JH, Yang ZF, Wang N, Wang Y, Wang LG. DMTF-GAN: a dual-branch mapping GAN with transformer for few-shot hyperspectral image classification. *IEEE J Sel Top Appl Earth Obs Remote Sens* **18**, 25654–25671 (2025);
17. Zhao BR, Zhang H, Wang YN, Jiang YM, Chen YR et al. Unleashing the potential of on-chip AI-powered hyperspectral hardware computing-A tutorial. *IEEE Trans Circuits Syst II-Express Briefs* **71**, 1733–1737 (2024);
18. George N, Singh H, Jotaniya R, Pandya SR. Raman spectroscopy for the determination of forensically important bio-fluids. *Forensic Sci Int* **340**, 111441 (2022);
19. Huang L, Lou XH, Wang HJ, Liu X, Zhou SW et al. Accelerating the Raman spectroscopic discrimination of normal and cancerous tissues with low-rank constraint. *Opt Commun* **586**, 131842 (2025);
20. Horgan CC, Bergholt MS, Thin MZ, Nagelkerke A, Kennedy R et al. Image-guided Raman spectroscopy probe-tracking for tumor margin delineation. *J Biomed Opt* **26**, 036002 (2021);
21. Shaker F, Monadjemi SA, Alirezaie J, Naghsh-Nilchi AR. A dictionary learning approach for human sperm heads classification. *Comput Biol Med* **91**, 181–190 (2017);
22. El-Melegy M, Mohamed D, ElMelegy T, Abdelrahman M. Identification of tuberculosis bacilli in ZN-stained sputum smear images: a deep learning approach. In *2019 IEEE/CVF Conference on Computer Vision and Pattern Recognition Workshops* 1131–1137 (IEEE, 2019); http://doi.org/10.1109/CVPRW.2019.00147.
23. Ji QB, Li X, Qu ZY, Dai C. Research on urine sediment images recognition based on deep learning. *IEEE Access* **7**, 166711–166720 (2019);
24. Nkamgang OT, Tchiotsop D, Tchinda BS, Fotsin HB. A neuro-fuzzy system for automated detection and classification of human intestinal parasites. *Inform Med Unlocked* **13**, 81–91 (2018);
25. Zhang XH, Jiang LQ, Yang DX, Yan JY, Lu XH. Correction to: urine sediment recognition method based on multi-view deep residual learning in microscopic image. *J Med Syst* **44**, 84 (2020);
26. Vaickus LJ, Suriawinata AA, Wei JW, Liu XY. Automating the Paris System for urine cytopathology—A hybrid deep-learning and morphometric approach. *Cancer Cytopathol* **127**, 98–115 (2019);
27. Nojima S, Terayama K, Shimoura S, Hijiki S, Nonomura N et al. A deep learning system to diagnose the malignant potential of urothelial carcinoma cells in cytology specimens. *Cancer Cytopathol* **129**, 984–995 (2021);
28. Tsuneki M, Abe M, Kanavati F. Deep learning-based screening of urothelial carcinoma in whole slide images of liquid-based cytology urine specimens. *Cancers* **15**, 226 (2023).
29. Wu SX, Shen RN, Hong GB, Luo Y, Wan H et al. Development and validation of an artificial intelligence-based model for detecting urothelial carcinoma using urine cytology images: a multicentre, diagnostic study with prospective validation. *eClinicalMedicine* **71**, 102566 (2024);
30. Naznine M, Salam A, Khan MM, Nobi SF, Chowdhury MEH. An ensemble deep learning approach for accurate urinary sediment detection using YOLOv9e and KD-YOLOX-ViT. *IEEE Access* **13**, 101934–101954 (2025);
31. Li QL, Li SY, Liu XY, He ZY, Wang T et al. FecalNet: automated detection of visible components in human feces using deep learning. *Med Phys* **47**, 4212–4222 (2020);
32. Tchinda BS, Noubom M, Tchiotsop D, Louis-Dorr V, Wolf D. Towards an automated medical diagnosis system for intestinal parasitosis. *Inf Med Unlocked* **13**, 101–111 (2018);
33. Yang A, Bakhtari N, Langdon-Embry L, Redwood E, Grandjean Lapierre S et al. Kankanet: an artificial neural network-based object detection smartphone application and mobile microscope as a point-of-care diagnostic aid for soil-transmitted helminthiases. *PLoS Negl Trop Dis* **13**, e0007577 (2019);
34. Dacal E, Bermejo-Peláez D, Lin L, Álamo E, Cuadrado D et al. Mobile microscopy and telemedicine platform assisted by deep learning for the quantification of *Trichuris trichiura* infection. *PLoS Negl Trop Dis* **15**, e0009677 (2021);
35. Mathison BA, Kohan JL, Walker JF, Smith RB, Ardon O et al. Detection of intestinal protozoa in trichrome-stained stool specimens by use of a deep convolutional neural network. *J Clin Microbiol* **58**, e02053–19 (2020);
36. Lee CC, Huang PJ, Yeh YM, Li PH, Chiu CH et al. Helminth egg analysis platform (HEAP): an opened platform for microscopic helminth egg identification and quantification based on the integration of deep learning architectures. *J Microbiol Immunol Infect* **55**, 395–404 (2022);
37. Thanchomnang T, Chaibutr N, Maleewong W, Janwan P. Automatic detection of *Opisthorchis viverrini* egg in stool examination using convolutional-based neural networks. *PeerJ* **12**, e16773 (2024);
38. Soli MAT, Agyei D, Bandawu WU, Boante LM, Appati JK. A modified hierarchical vision transformer model for poultry disease detection. *IET Image Process* **19**, e70115 (2025);
39. Mithra KS, Sam Emmanuel WR. Automated identification of mycobacterium bacillus from sputum images for tuberculosis diag-

nosis. *Signal, Image Video Process* **13**, 1585–1592 (2019);
40. Chithra RS, Jagatheeswari P. Severity detection and infection level identification of tuberculosis using deep learning. *Int J Imaging Syst Technol* **30**, 994–1011 (2020);
41. Hu MY, Liu YQ, Zhang YX, Guan T, He YH. Automatic detection of tuberculosis bacilli in sputum smear scans based on subgraph classification. In *2019 International Conference on Medical Imaging Physics and Engineering* 1–7 (IEEE, 2019); http://doi.org/10.1109/ICMIPE47306.2019.9098210.
42. Zachariou M, Arandjelović O, Sabiiti W, Mtafya B, Sloan D. Tuberculosis bacteria detection and counting in fluorescence microscopy images using a multi-stage deep learning pipeline. *Information* **13**, 96 (2022).
43. Zachariou M, Arandjelović O, Dombay E, Sabiiti W, Mtafya B et al. Localization and phenotyping of tuberculosis bacteria using a combination of deep learning and SVMs. *Comput Biol Med* **167**, 107573 (2023);
44. Miahi E, Mirroshandel SA, Nasr A. Genetic Neural Architecture Search for automatic assessment of human sperm images. *Expert Syst Appl* **188**, 115937 (2022);
45. Abbasi A, Miahi E, Mirroshandel SA. Effect of deep transfer and multi-task learning on sperm abnormality detection. *Comput Biol Med* **128**, 104121 (2021);
46. Ilhan HO, Serbes G. Sperm morphology analysis by using the fusion of two-stage fine-tuned deep networks. *Biomed Signal Process Control* **71**, 103246 (2022);
47. Zou SJ, Li C, Sun H, Xu PZ, Zhang J et al. TOD-CNN: an effective convolutional neural network for tiny object detection in sperm videos. *Comput Biol Med* **146**, 105543 (2022);
48. Yang H, Ma MM, Chen XF, Chen GW, Shen Y et al. Multidimensional morphological analysis of live sperm based on multiple-target tracking. *Comput Struct Biotechnol J* **24**, 176–184 (2024);
49. Turkoglu AK, Serbes G, Uzun H, Aktas A, Yigit MH et al. Category-aware two-stage divide-and-ensemble framework for sperm morphology classification. *Diagnostics* **15**, 2234 (2025);
50. Alva A, Cangalaya C, Quiliano M, Krebs C, Gilman RH et al. Mathematical algorithm for the automatic recognition of intestinal parasites. *PLoS One* **12**, e0175646 (2017);
51. Li ZX, Gong HL, Zhang W, Chen L, Tao JC et al. A robust and automatic method for human parasite egg recognition in microscopic images. *Parasitol Res* **114**, 3807–3813 (2015);
52. Liu L, Yuan Y, Zhang J, Lei HT, Wang Q et al. Automatic identification of fungi under complex microscopic fecal images. *J Biomed Opt* **20**, 076004 (2015);
53. Wang W, Si MM, Chen FQ, Liu H, Jiang XM. Study on recognition method of label-free red and white cell using fecal microscopic image. In *Proceedings of the 2018 6th International Conference on Bioinformatics and Computational Biology* 95–100 (ACM, 2018); http://doi.org/10.1145/3194480.3198909.
54. Wang XZ, Liu L, Du XH, Zhang J, Liu JX et al. Leukocyte recognition in human fecal samples using texture features. *J Opt Soc Am A* **35**, 1941–1948 (2018);
55. Govindan L, Padmasini N, Yacin M. Automated tuberculosis screening using Zeihl Neelson image. In *2015 IEEE International Conference on Engineering and Technology* 1–4 (IEEE, 2015); http://doi.org/10.1109/ICETECH.2015.7275031.
56. Rulaningtyas R, Bayu Suksmono A, Mengko T, Saptawati P. Multi patch approach in K-means clustering method for color image segmentation in pulmonary tuberculosis identification. In *2015 4th International Conference on Instrumentation, Communications, Information Technology, and Biomedical Engineering* 75–78 (IEEE, 2015); http://doi.org/10.1109/ICICI-BME.2015.7401338.
57. Ayma V, De Lamare R, Castañeda B. An adaptive filtering approach for segmentation of tuberculosis bacteria in Ziehl-Neelsen sputum stained images. In *2015 Latin America Congress on Computational Intelligence* 1–5 (IEEE, 2015); http://doi.org/10.1109/LA-CCI.2015.7435964.
58. Shwetha V, Prasad K, Mukhopadhyay C, Banerjee B, Chakrabarti A. Automatic detection of bacilli bacteria from Ziehl-Neelsen sputum smear images. In *2021 2nd International Conference on Communication, Computing and Industry 4. 0* 1–5 (IEEE, 2021); http://doi.org/10.1109/C2I454156.2021.9689283.
59. Zou YL, Bu H, Guo L, Liu YJ, He JY et al. Staining with two observational methods for the diagnosis of tuberculous meningitis. *Exp Ther Med* **12**, 3934–3940 (2016);
60. Ilhan HO, Serbes G, Aydin N. Automated sperm morphology analysis approach using a directional masking technique. *Comput Biol Med* **122**, 103845 (2020);
61. Li CJ, Han HZ, Hu ZW, Zhang CM, Zhi EL. Improved one-stage algorithm with attention fusion for human sperm detection based on deep learning. In *Proceedings of the 7th International Conference on Life System Modeling and Simulation Intelligent Life System Modelling, Image Processing and Analysis* 232–241 (Springer, 2021); http://doi.org/10.1007/978-981-16-7207-1_23.
62. Dinesh Jackson Samuel R, Rajesh Kanna B. RETRACTED ARTICLE: tuberculosis (TB) detection system using deep neural networks. *Neural Computi Appl* **31**, 1533–1545 (2019);
63. Baykal E, Dogan H, Ercin ME, Ersoz S, Ekinci M. Modern convolutional object detectors for nuclei detection on pleural effusion cytology images. *Multimed Tools Appl* **79**, 15417–15436 (2020);
64. Li FQ, Wang SL, Wang ZH. Protecting deep cerebrospinal fluid cell image processing models with backdoor and semi-distillation. In *2021 Digital Image Computing: Techniques and Applications* 1–7 (IEEE, 2021); http://doi.org/10.1109/DICTA52665.2021.9647115.
65. Yu WJ, Liu YY, Zhao YS, Huang HF, Liu JH et al. Deep learning-based classification of cancer cell in leptomeningeal metastasis on cytomorphologic features of cerebrospinal fluid. *Front Oncol* **12**, 821594 (2022);
66. Baykal Kablan E, Dogan H, Ercin ME, Ersoz S, Ekinci M. An ensemble of fine-tuned fully convolutional neural networks for pleural effusion cell nuclei segmentation. *Comput Electr Eng* **81**, 106533 (2020);
67. Xie XF, Fu CC, Lv L, Ye QY, Yu Y et al. Deep convolutional neural network-based classification of cancer cells on cytological pleural effusion images. *Mod Pathol* **35**, 609–614 (2022);
68. Ren WH, Zhu YL, Wang Q, Jin HZ, Guo YY et al. Deep learning-based classification and targeted gene alteration prediction from pleural effusion cell block whole-slide images. *Cancers* **15**, 752 (2023).
69. Tian ZK, Peng DL, Wang DD, Zhang LN, Zou Z et al. A Swin Transformer based on multi-directional-shift window attention and inductive bias for diagnosis of pleural effusion. *Appl Soft Comput* **177**, 113146 (2025);
70. Su F, Sun Y, Hu YJ, Yuan PJ, Wang XY et al. Development and validation of a deep learning system for ascites cytopathology interpretation. *Gastric Cancer* **23**, 1041–1050 (2020);
71. Kim HK, Han E, Lee J, Yim K, Abdul-Ghafar J et al. Artificial-intelligence-assisted detection of metastatic colorectal cancer cells in ascitic fluid. *Cancers* **16**, 1064 (2024).
72. Tian F, Liu D, Wei N, Fu QQ, Sun L et al. Prediction of tumor origin in cancers of unknown primary origin with cytology-based deep learning. *Nat Med* **30**, 1309–1319 (2024);
73. Schweizer L, Seegerer P, Kim HY, Saitenmacher R, Muench A et al. Analysing cerebrospinal fluid with explainable deep learning: from diagnostics to insights. *Neuropathol Appl Neurobiol* **49**, e12866 (2023);
74. Zhang DJ, Cheng ZY, Song YL, Li HD, Shi L et al. Rapid and sensitive acute leukemia classification and diagnosis platform using deep learning-assisted SERS detection. *Cell Rep Med* **6**, 102320 (2025);
75. Saikia AR, Bora K, Mahanta LB, Das AK. Comparative assessment of CNN architectures for classification of breast FNAC images. *Tissue Cell* **57**, 8–14 (2019);
76. Miselis B, Fevens T, Krzyżak A, Kowal M, Monczak R. Deep neural networks for breast cancer diagnosis: fine needle biopsy scenario.

In Korbicz J, Maniewski R, Patan K, Kowal M. *Current Trends in Biomedical Engineering and Bioimages Analysis* 131–142 (Springer, Cham, 2020); http://doi.org/10.1007/978-3-030-29885-2_12.
77. Zerouaoui H, Idri A, Nakach FZ, El Hadri R. Breast fine needle cytological classification using deep hybrid architectures. In *Proceedings of the 21st International Conference on Computational Science and Its Applications* 186–202 (Springer, 2021); http://doi.org/10.1007/978-3-030-86960-1_14.
78. Bal A, Das M, Satapathy SM, Jena M, Das SK. Automated diagnosis of breast cancer with roi detection using YOLO and heuristics. In *Proceedings of the 17th International Conference on Distributed Computing and Internet Technology* 253–267 (Springer, 2021); http://doi.org/10.1007/978-3-030-65621-8_16.
79. Bal A, Das M, Satapathy SM, Jena M, Das SK. BFCNet: a CNN for diagnosis of ductal carcinoma in breast from cytology images. *Pattern Anal Appl* **24**, 967–980 (2021);
80. Abdallah A, Kasem MS, Abdelhalim I, Alghamdi NS, El-Baz A. Improving BI-RADS mammographic classification with self-supervised vision transformers and cascade learning. *IEEE Access* **13**, 135500–135514 (2025);
81. Sanyal P, Mukherjee T, Barui S, Das A, Gangopadhyay P. Artificial intelligence in cytopathology: a neural network to identify papillary carcinoma on thyroid fine-needle aspiration cytology smears. *J Pathol Inform* **9**, 43 (2018);
82. Guan Q, Wang YJ, Ping B, Li DS, Du JJ et al. Deep convolutional neural network VGG-16 model for differential diagnosing of papillary thyroid carcinomas in cytological images: a pilot study. *J Cancer* **10**, 4876–4882 (2019);
83. Duc NT, Lee YM, Park JH, Lee B. An ensemble deep learning for automatic prediction of papillary thyroid carcinoma using fine needle aspiration cytology. *Expert Syst Appl* **188**, 115927 (2022);
84. Zhang JZ, Zhang HL, Jiang P, Huang Q, Zhu GY et al. High efficiency classification of thyroid cytopathological images based on knowledge distillation and vision transformer. *Sci Rep* **15**, 30059 (2025);
85. Tsukamoto T, Teramoto A, Yamada A, Kiriyama Y, Sakurai E et al. Comparison of fine-tuned deep convolutional neural networks for the automated classification of lung cancer cytology images with integration of additional classifiers. *Asian Pac J Cancer Prev* **23**, 1315–1324 (2022);
86. Teramoto A, Kiriyama Y, Tsukamoto T, Sakurai E, Michiba A et al. Weakly supervised learning for classification of lung cytological images using attention-based multiple instance learning. *Sci Rep* **11**, 20317 (2021);
87. Ai D, Hu Q, Chao YC, Fu CC, Yuan W et al. Artificial intelligence-based rapid on-site cytopathological evaluation for bronchoscopy examinations. *Intell-Based Med* **6**, 100069 (2022);
88. Lin CK, Chang J, Huang CC, Wen YF, Ho CC et al. Effectiveness of convolutional neural networks in the interpretation of pulmonary cytologic images in endobronchial ultrasound procedures. *Cancer Med* **10**, 9047–9057 (2021);
89. Momeni-Boroujeni A, Yousefi E, Somma J. Computer-assisted cytologic diagnosis in pancreatic FNA: an application of neural networks to image analysis. *Cancer Cytopathol* **125**, 926–933 (2017);
90. Zhang S, Zhou YF, Tang DH, Ni MH, Zheng JY et al. A deep learning-based segmentation system for rapid onsite cytologic pathology evaluation of pancreatic masses: a retrospective, multicenter, diagnostic study. *eBioMedicine* **80**, 104022 (2022);
91. Hussain E, Mahanta LB, Das CR, Talukdar RK. A comprehensive study on the multi-class cervical cancer diagnostic prediction on pap smear images using a fusion-based decision from ensemble deep convolutional neural network. *Tissue Cell* **65**, 101347 (2020);
92. Wang RQ, Armin MA, Denman S, Petersson L, Ahmedt-Aristizabal D. Towards interpretable attention networks for cervical cancer analysis. In *2021 43rd Annual International Conference of the IEEE Engineering in Medicine & Biology Society* 3613–3616 (IEEE, 2021); http://doi.org/10.1109/EMBC46164.2021.9629604.
93. Gao WJ, Xu CY, Li G, Zhang Y, Bai NL et al. Cervical cell image classification-based knowledge distillation. *Biomimetics* **7**, 195 (2022),
94. Rahaman M, Li C, Yao YD, Kulwa F, Wu XC et al. DeepCervix: a deep learning-based framework for the classification of cervical cells using hybrid deep feature fusion techniques. *Comput Biol Med* **136**, 104649 (2021);
95. Ghoneim A, Muhammad G, Hossain MS. Cervical cancer classification using convolutional neural networks and extreme learning machines. *Future Gener Comput Syst* **102**, 643–649 (2020);
96. Zhu XH, Li XM, Ong K, Zhang WL, Li WC et al. Hybrid AI-assistive diagnostic model permits rapid TBS classification of cervical liquid-based thin-layer cell smears. *Nat Commun* **12**, 3541 (2021);
97. Cheng SH, Liu SB, Yu JY, Rao G, Xiao YW et al. Robust whole slide image analysis for cervical cancer screening using deep learning. *Nat Commun* **12**, 5639 (2021);
98. Zhang Z, Yao P, Chen MX, Zeng L, Shao PF et al. SCAC: a semi-supervised learning approach for cervical abnormal cell detection. *IEEE J Biomed Health Inform* **28**, 3501–3512 (2024);
99. Nirmala G, Nayudu PP, Kumar AR, Sagar R. Automatic cervical cancer classification using adaptive vision transformer encoder with CNN for medical application. *Pattern Recognit* **160**, 111201 (2025);
100. Litjens G, Kooi T, Bejnordi BE, Setio AAA, Ciompi F et al. A survey on deep learning in medical image analysis. *Med Image Anal* **42**, 60–88 (2017);
101. Bengtsson E, Malm P. Screening for cervical cancer using automated analysis of PAP-smears. *Comput Math Methods in Med* **2014**, 842037 (2014);
102. Teramoto A, Yamada A, Kiriyama Y, Tsukamoto T, Yan K et al. Automated classification of benign and malignant cells from lung cytological images using deep convolutional neural network. *Inform Med Unlocked* **16**, 100205 (2019);
103. Yamada R, Nakane K, Kadoya N, Matsuda C, Imai H et al. Development of “mathematical technology for cytopathology, ” an image analysis algorithm for pancreatic cancer. *Diagnostics* **12**, 1149 (2022),
104. Khan SU, Islam N, Jan Z, Din IU, Khan A et al. An e-Health care services framework for the detection and classification of breast cancer in breast cytology images as an IoMT application. *Future Gener Comput Syst* **98**, 286–296 (2019);
105. Zhao BD, Deng WL, Li ZH, Zhou C, Gao ZH et al. LESS: label-efficient multi-scale learning for cytological whole slide image screening. *Med Image Anal* **94**, 103109 (2024);
106. Gopinath B, Shanthi N. Computer-aided diagnosis system for classifying benign and malignant thyroid nodules in multi-stained FNAB cytological images. *Australas Phys Eng Sci Med* **36**, 219–230 (2013);
107. Gopinath B, Shanthi N. Support vector machine based diagnostic system for thyroid cancer using statistical texture features. *Asian Pac J Cancer Prev* **14**, 97–102 (2013);
108. Mitra S, Dey S, Das N, Chakrabarty S, Nasipuri M et al. Identification of benign and malignant cells from cytological images using superpixel based segmentation approach. In *Proceedings of the 52nd Annual Convention of the Computer Society of India Social Transformation – Digital Way* 257–269 (Springer, 2018); http://doi.org/10.1007/978-981-13-1343-1_24.
109. Teramoto A, Tsukamoto T, Yamada A, Kiriyama Y, Imaizumi K et al. Deep learning approach to classification of lung cytological images: two-step training using actual and synthesized images by progressive growing of generative adversarial networks. *PLoS One* **15**, e0229951 (2020);
110. Sun RN, Pang YX, Li WF. Efficient lung cancer image classification and segmentation algorithm based on an improved swin transformer. *Electronics* **12**, 1024 (2023);
111. Thosani N, Patel J, Moreno V, Bhakta D, Patil P et al. 77 Develop-

ment and validation of artificial intelligence based rapid onsite cytopathology evaluation (Rose-Aid™) for endoscopic ultrasound-guided fine-needle aspiration (EUS-FNA) of pancreatic solid lesions. *Gastroenterology* **160**, S–17 (2021);
112. Eltabbakh GH, Trask CE. Scrape cytology for intraoperative evaluation of lymph nodes in gynecologic cancer. *Obstet Gynecol* **95**, 67–71 (2000);
113. Nangia A, Sehgal S, Chander R. Scrape cytology in localized oral mucosal leishmaniasis. *J Cytol* **31**, 180–181 (2014);
114. Nayar R, Wilbur DC. The pap test and Bethesda 2014: “The reports of my demise have been greatly exaggerated. ” (after a quotation from Mark Twain). *Acta Cytol* **59**, 121–132 (2015);
115. Bao HL, Bi H, Zhang XS, Zhao Y, Dong Y et al. Artificial intelligence-assisted cytology for detection of cervical intraepithelial neoplasia or invasive cancer: a multicenter, clinical-based, observational study. *Gynecol Oncol* **159**, 171–178 (2020);
116. Holmström O, Linder N, Kaingu H, Mbuuko N, Mbete J et al. Point-of-care digital cytology with artificial intelligence for cervical cancer screening in a resource-limited setting. *JAMA Netw Open* **4**, e211740 (2021);
117. Tan XY, Li KX, Zhang JC, Wang WZ, Wu B et al. Automatic model for cervical cancer screening based on convolutional neural network: a retrospective, multicohort, multicenter study. *Cancer Cell Int* **21**, 35 (2021);
118. Ke J, Shen YQ, Lu YZ, Deng JW, Wright JD et al. Quantitative analysis of abnormalities in gynecologic cytopathology with deep learning. *Lab Invest* **101**, 513–524 (2021);
119. Kermany DS, Goldbaum M, Cai WJ, Valentim CCS, Liang HY et al. Identifying medical diagnoses and treatable diseases by image-based deep learning. *Cell* **172**, 1122–1131.e9 (2018);
120. Chen XX, Wang XM, Zhang K, Fung KM, Thai TC et al. Recent advances and clinical applications of deep learning in medical image analysis. *Med Image Anal* **79**, 102444 (2022);
121. Marletta S, Treanor D, Eccher A, Pantanowitz L. Whole-slide imaging in cytopathology: state of the art and future directions. *Diagn Histopathol* **27**, 425–430 (2021);
122. Yao KL, Sadimin E, Chang SE, Schmolze D, Li ZB. Current applications and challenges of digital pathology in cytopathology. *Hum Pathol Rep* **28**, 300634 (2022);
123. Awan R, Benes K, Azam A, Song TH, Shaban M et al. Deep learning based digital cell profiles for risk stratification of urine cytology images. *Cytometry Part A* **99**, 732–742 (2021);
124. Bankhead P, Loughrey MB, Fernández JA, Dombrowski Y, McArt DG et al. QuPath: open source software for digital pathology image analysis. *Sci Rep* **7**, 16878 (2017);
125. Guan H, Liu MX. Domain adaptation for medical image analysis: a survey. *IEEE Trans Biomed Eng* **69**, 1173–1185 (2022);
126. Hong Y, Zhu WP. Spatial co-training for semi-supervised image classification. *Pattern Recognit Lett* **63**, 59–65 (2015);
127. Xia YD, Yang D, Yu ZD, Liu FZ, Cai JZ et al. Uncertainty-aware multi-view co-training for semi-supervised medical image segmentation and domain adaptation. *Med Image Anal* **65**, 101766 (2020);
128. Zhao SQ, He YJ, Qin J, Wang ZX. A semi-supervised deep learning method for cervical cell classification. *Anal Cell Pathol* **2022**, 4376178 (2022);
129. Zheng X, Wang Y, Wang GY, Liu JG. Fast and robust segmentation of white blood cell images by self-supervised learning. *Micron* **107**, 55–71 (2018);
130. Guo YY, Wang X, Xiao PC, Xu XZ. An ensemble learning framework for convolutional neural network based on multiple classifiers. *Soft Comput* **24**, 3727–3735 (2020);
131. Gui J, Zhang HZ. Learning rates for multi-task regularization networks. *Neurocomputing* **466**, 243–251 (2021);
132. Elsken T, Metzen JH, Hutter F. Neural architecture search: a survey. *J Mach Learn Res* **20**, 1997–2017 (2019).
133. Yu MK, Ma JZ, Fisher J, Kreisberg JF, Raphael BJ et al. Visible machine learning for biomedicine. *Cell* **173**, 1562–1565 (2018);
134. Balasubramaniam S, Chirchi V, Kadry S, Agoramoorthy M, Senthilvel PG et al. The road ahead: emerging trends, unresolved issues, and concluding remarks in generative AI-a comprehensive review. *Int J Intell Syst* **2024**, 4013195 (2024);

Acknowledgements

The authors thank the financial support from the National Natural Science Foundation of China (62501111, 62122017), Postdoctoral Fellowship Program of CPSF (GZB20240123), National Key R&D Program of China (grant no.2023YF0724300).

Author contributions

Jiuchuan Guo: Writing – review & iting, Writing – original draft, Literature management. Ziyan Yin: Writing – review & editing, Visualization. Lanqing Zeng: Writing – review & editing, Conceptualization. Hongyu Li: Literature management. Yusheng Fu: Supervision. Renting Liu: Supervision. Jinhong Guo: Supervision, Funding acquisition.

Competing interests

The authors declare no competing financial interests.

Open Access This article is licensed under a Creative Commons Attribution 4.0 International License, which permits use, sharing, adaptation, distribution and reproduction in any medium or format, as long as you give appropriate credit to the original author(s) and the source, provide a link to the Creative Commons license, and indicate if changes were made. To view a copy of this license, visit http://creativecommons.org/licenses/by/4.0/
©The Author(s) 2026.

Opto-Electronic Journals Group
www.oejournal.org
Scan for Article PDF